

Propene/Ethene-[1-¹³C] Copolymerization as a Tool for Investigating Catalyst Regioselectivity. 2. The MgCl₂/TiCl₄–AlR₃ System

Vincenzo Busico,* Roberta Cipullo, Carmen Polzone, and Giovanni Talarico

Dipartimento di Chimica, Università di Napoli Federico II, Via Cintia, 80126 Naples, Italy

John C. Chadwick†

Dutch Polymer Institute, Laboratory of Polymer Chemistry, Eindhoven University of Technology, P.O. Box 513, 5600 MB Eindhoven, The Netherlands

Received February 1, 2003; Revised Manuscript Received February 26, 2003

ABSTRACT: The propene/ethene-[1-¹³C] copolymerization method has been applied to measure precisely the regioselectivity in propene polymerization of the “simple” MgCl₂/TiCl₄ catalyst (activated with Al(ⁱ-Bu)₃), which can be viewed as the ancestor of all present-day MgCl₂-supported industrial catalysts containing Lewis bases as selective modifiers. It has been found that the average content of 2,1-regiomistakes in the polypropylene produced is fairly high (ca. 0.7 mol %), although—not unexpectedly, due to the multisite catalyst nature—these are distributed rather nonuniformly throughout the polymer. The difficulty in detecting the 2,1-units, despite their relatively high concentration, in the ¹³C NMR spectra of homopolymer samples at natural ¹³C abundance has been traced to their occurrence in a variety of stereochemical environments, which leads to splitting and broadening of the corresponding resonances. The fraction of “dormant” polypropylene chains with a 2,1-last-inserted unit was estimated to be in the 20–50% range. QM calculations of regioselectivity on classical Corradini-type models of epitactic octahedral catalytic Ti species turned out to be in basic agreement with the experiment.

Introduction

Terms like “exceedingly high”, “extreme”, or even “complete”, referring to the selectivity of a chemical process are not uncommon. Of course, they must not be taken in a literal sense but instead interpreted for what they really imply, i.e., that the reaction does not lead to side products *in appreciable amounts*. In turn, what “*appreciable*” means is heavily dependent on the context and, in particular, on the analytical tool(s) used to sample the reaction products and/or on the way these are used. In most cases, such terms are acceptable, despite their relative meaning. When, however, one or more side products can act as a “poison” (in the most general acceptance of the term), their quantitative determination down to trace amounts becomes of crucial importance.

In part 1 of this series,¹ we introduced and calibrated a method to improve the sensitivity of the ¹³C NMR measurements of regioselectivity for transition-metal-assisted propene polymerizations. In brief, catalysts which strongly favor 1,2-propene enchainment are known² to be partly inhibited by the occasional 2,1-regiomistakes, which introduce a high steric hindrance at the active metal centers and slow a subsequent propene insertion by a factor typically in the range of 100 to 1000. This makes the precise evaluation of the regioselectivity a precondition for understanding the overall polymerization kinetics. Not surprisingly, when ethene is also present in the reaction medium, already at low concentration it reacts much faster than propene with the “dormant” chains; therefore, “all” 2,1-last-inserted propene insertions are followed by ethene ones, and the copolymer ethene units flanked by propene units in opposite enchainments are effective markers

of the regiomistakes. By using ethene-[1-¹³C] in the place of ethene at natural isotopic abundance, the sensitivity of the ¹³C NMR analysis is increased by a factor of 50, and the threshold for the detection of the regiomistakes decreased accordingly (from 0.1–1.0 to 0.002–0.02 mol %, respectively).¹

Thanks to this method, we were able to give a precise meaning to the otherwise vague concept of “extremely regioselective” previously referred to a number of metallocene catalysts, e.g., Cp₂TiCl₂ (1 regioinversion out of 10 000);³ Cp₂ZrCl₂ and Me₂SiCp₂ZrCl₂ (2–3 regioinversions out of 1000);³ Ph₂C(Cp)(9-Fluorenyl)ZrCl₂ (8 regioinversions out of 10 000).⁴ We have now extended our approach to heterogeneous multisite Ziegler–Natta catalysts, in particular to MgCl₂-supported ones, which are also commonly referred to as exceedingly regioselective in favor of 1,2-insertion.^{5,6} In the present paper, we report the results obtained for the “parent” system MgCl₂/TiCl₄–AlR₃; in a following one, we will then discuss the case of systems of industrial use, containing Lewis bases as selective modifiers.^{5,6}

The “simple” MgCl₂/TiCl₄ catalyst was developed in the early 1970s,^{5,6} as a result of the search for an inert carrier of TiCl₄ species enabling a more effective utilization of Ti compared with “violet” TiCl₃. Although serendipitous in origin, the identification of MgCl₂ as an elective matrix for the epitactic chemisorption of TiCl₄ and its subsequent reduction/alkylation by means of the AlR₃ cocatalyst has now solid theoretical foundations.^{6,7} It is generally accepted that a variety of active site precursors can form on the coordinatively unsaturated 100 and 110 side edges of the MgCl₂ plateletlike crystals and that only a relatively small fraction of them possesses the steric requirements for evolving to catalytic species of high enantioselectivity.^{6,7} As a matter of fact, the polypropylene produced is poorly stereoregular, and only 30–50 wt % is insoluble in boiling

* Corresponding author. E-mail: busico@chemistry.unina.it.

† On secondment from Basell Polyolefins.

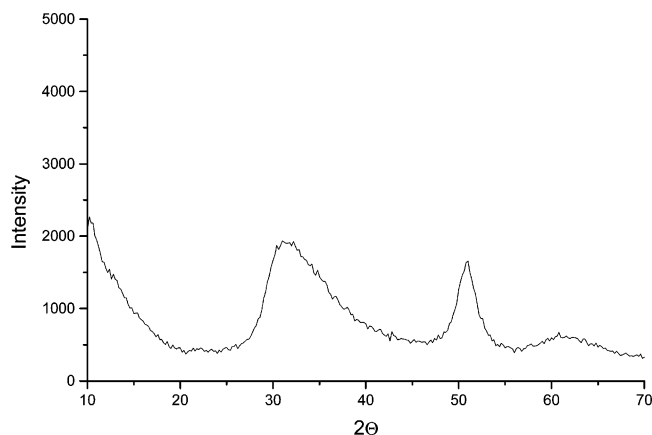


Figure 1. Powder X-ray diffraction spectrum of the $\text{MgCl}_2/\text{TiCl}_4$ catalyst sample (Ni-filtered $\text{Cu K}\alpha$ radiation).

Table 1. List of the Propene/Ethene-[1-¹³C] Copolymerization Experiments in the Presence of Catalyst System $\text{MgCl}_2/\text{TiCl}_4\text{-Al}(\text{iBu})_3$ at 50 °C

run/sample no.	$[\text{E}]/[\text{P}] \times 10^3$ ^a	E (mol %) ^b	"isotactic" fraction (wt %)	[<i>mmmm</i>] (%)
PP1	0	0	43 ^c	85.9
EP5	0.33	0.521(15)	43 ^d	85.3 ^e
EP3	0.72	0.941(12)	45 ^d	86.4 ^e
EP2	1.43	1.63(24)	45 ^d	86.4 ^e
EP7	2.68	2.61(11)	44 ^d	85.9 ^e

^a In the liquid phase; E = ethene-[1-¹³C] and P = propene.

^b Ethene incorporation in the copolymer. ^c Fraction insoluble in boiling heptane. ^d Fraction insoluble in boiling hexane. ^e Referred to the propene homosequences.

heptane and as such deserves the conventional definition of "isotactic".⁵⁻⁷

This notwithstanding, the catalyst is highly regioselective. ¹³C NMR fails to detect regioirregular enchainments in the "isotactic" polymer fraction, whereas low amounts (<1 mol %) of isolated 2,1-units, difficult to quantify more precisely due to the poor signal-to-noise ratio, can be observed in the spectra of "less-tactic" (e.g., xylene- or boiling-heptane-soluble) fractions.^{6,8}

Results and Discussion

(i) Experimental Studies. The $\text{MgCl}_2/\text{TiCl}_4$ catalyst batch used in this study was prepared by reaction of a $\text{Mg}(\text{Bu})_2$ solution in hexane with dry $\text{HCl}(\text{g})$, followed by impregnation of the highly activated MgCl_2 precipitate with TiCl_4 (see Experimental Section). The resulting $\text{MgCl}_2/\text{TiCl}_4$ adduct is characterized by extremely small primary particles, as is clearly apparent from the powder X-ray diffraction spectrum (Figure 1); a line-shape analysis performed on the profile of a similarly prepared sample ended up with an average size of the hexagonal plateletlike crystals of ≈ 5 unit cells (≈ 20 Å) along the side edges and a thickness of 1–2 structural layers only.⁹

Propene/ethene-[1-¹³C] copolymerizations (Table 1) were carried out at 50 °C, using $\text{Al}(\text{iBu})_3$ as the cocatalyst (AlEt_3 was avoided because it is known to liberate ethene by β -H elimination). The copolymers were characterized by ¹³C NMR, both as obtained and after solvent fractionation, to separate an "isotactic" from a "less-tactic" part. For a propene homopolymer, as already noted, the divide is usually set by Kumagawa extraction with boiling heptane;⁵⁻⁷ in the case of lower-melting semicrystalline propene/ethene copolymers, on the other hand, a lower-boiling solvent needs to be used.

Table 2. Results of the ¹³C NMR Characterization of the Propene/Ethene-[1-¹³C] Copolymers in Table 1

sample no.	$[\text{E}]/[\text{P}] \times 10^3$ ^a	Q_E (mol %) ^b	Q_{SE} (mol %) ^c	k_1 ^d
Raw Samples				
EP5	0.33	0.521(15)	0.096(15)	0.72(7)
EP3	0.72	0.941(12)	0.145(4)	
EP2	1.43	1.63(24)	0.207(24)	
EP7	2.68	2.61(11)	0.298(13)	
"Isotactic" Fractions				
EP5	0.33	0.305(15)	0.034(5)	0.19(4)
EP3	0.72	0.550(5)	0.057(3)	
EP2	1.43	0.881(5)	0.067(4)	
EP7	2.68	1.47(6)	0.100(4)	
"Less-Tactic" Fractions				
EP5	0.33	0.584(10)	0.106(10)	1.5(2)
EP3	0.72	1.21(12)	0.193(19)	
EP2	1.43	2.29(14)	0.320(20)	
EP7	2.68	4.10(7)	0.510(9)	

^a In the liquid phase; E = ethene-[1-¹³C] and P = propene.

^b Mole fraction of ethene-[1-¹³C] units in the copolymer. ^c Mole fraction of ethene-[1-¹³C] units following a 2,1 propene unit.

^d Extrapolated fraction of 2,1-insertions in propene homopolymerization (see text).

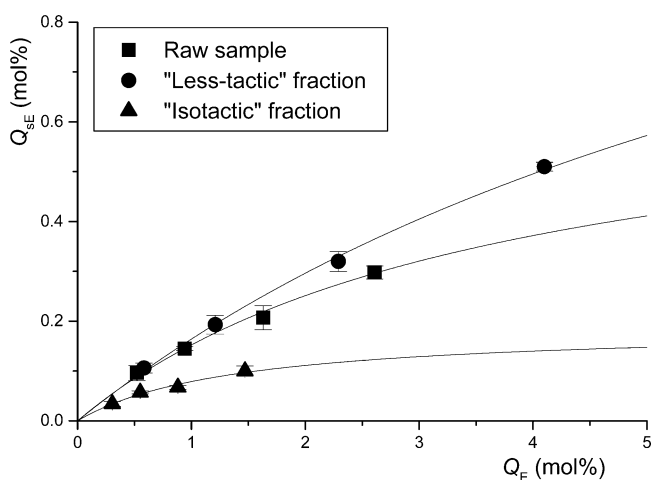


Figure 2. Mole fraction of ethene-[1-¹³C] units adjacent to a 2,1-propene unit (Q_{SE}) vs total ethene-[1-¹³C] content (Q_E) for the raw propene/ethene-[1-¹³C] copolymer samples and for their "isotactic" and "less-tactic" fraction (data from Table 2).

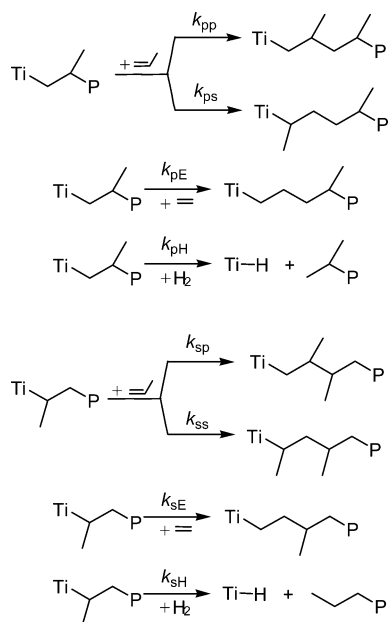
We opted for hexane because both the weight amount and the ¹³C NMR degree of stereoregularity of the propene homosequences for the hexane-insoluble copolymer fraction turned out to be very similar to the corresponding parameters for the heptane-insoluble homopolymer fraction (Table 1).

On all copolymers and fractions thereof, we measured the total amount of incorporated ethene-[1-¹³C] (Q_E), and the fraction found to be adjacent to a 2,1- (secondary) propene unit (Q_{SE}) (Table 2). Plots of Q_{SE} vs Q_E for the raw samples, and for their "isotactic" and "less-tactic" fractions, are reported in Figure 2. They all show the expected¹ asymptotic behavior, well-fitted by a simple saturation function:

$$Q_{SE} = k_1 Q_E / (k_2 + Q_E)$$

with the upper limit k_1 being the fraction of 2,1-insertions in propene homopolymerization (i.e., the ratio of kinetic constants k_{ps}/k_{pp} , Scheme 1). The best-fit values of k_1 are also given in Table 2; on average, $k_1 = 0.72$ mol %, but its distribution is very broad, as a consequence of the multisite catalyst nature, ranging

Scheme 1



from 0.19 mol % for the “isotactic” fraction to 1.5 mol % for the “less-tactic” one.

These values are higher than commonly assumed, and apparently inconsistent with the much lower estimates based on the ^{13}C NMR characterizations of homopolymers.^{6,8} To find a reason for this, let us first give a closer look at the ^{13}C NMR spectra of the “isotactic” and “less-tactic” fraction of a typical propene/ethene- $[1-^{13}\text{C}]$ copolymer ($Q_E = 0.94$ mol %), shown in Figure 3, parts A and B, respectively. The resonances of the $S_{\alpha\beta}$ C's of ethene- $[1-^{13}\text{C}]$ units between propene units with opposite enchainments are well-visible and explicitly labeled. For the “isotactic” fraction, they appear as three peaks, two of which at chemical shift values ($\delta = 34.53$ and 34.75 ppm) coincident with those in the spectra of similar copolymers prepared with isotactic-selective C_2 -symmetric *ansa*-metallocene catalysts¹ and attributed to C_a and C_b in the stereosequence of Chart 1A. We assign the third peak, at $\delta = 34.69$ ppm, to C_c in the stereosequence of Chart 1B. From spectral simulation, we estimated a ratio between the two structures as low as 1.6; this indicates that, despite the fairly high degree of isotacticity of the fraction, the 2,1-propene units are substantially stereoirregular. The pattern of the “less-tactic” fraction is obviously more complicated, due to the lower stereoregularity; indeed, the ethene- $[1-^{13}\text{C}]$ units adjacent to 2,1-propene ones give rise to complex multiplets in the regions of $\delta = 34.4\text{--}35.0$ ppm (including

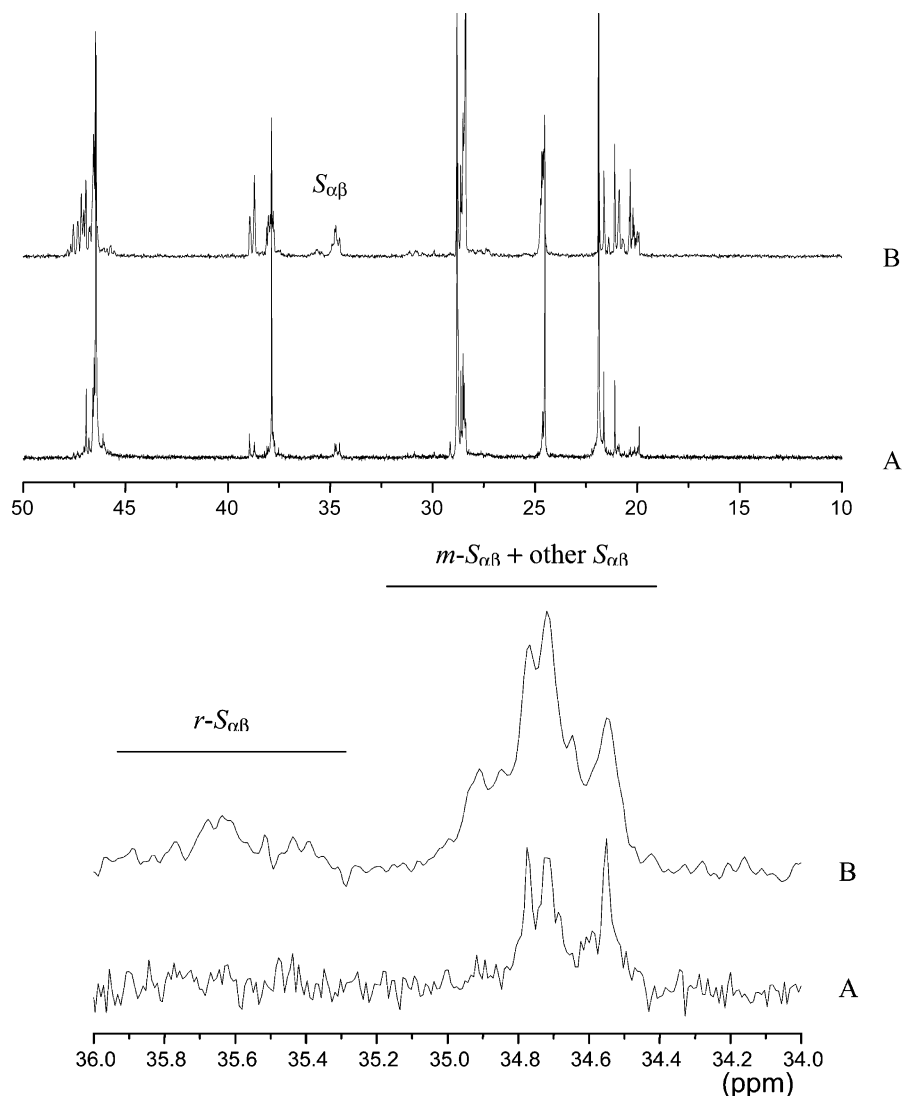


Figure 3. 50.3 MHz ^{13}C NMR spectra of the “isotactic” fraction (A) and of the “less-tactic” fraction (B) of a typical propene/ethene- $[1-^{13}\text{C}]$ copolymer (sample EP3 of Table 1). Key: top, total spectrum; bottom, detail of the $S_{\alpha\beta}$ region.

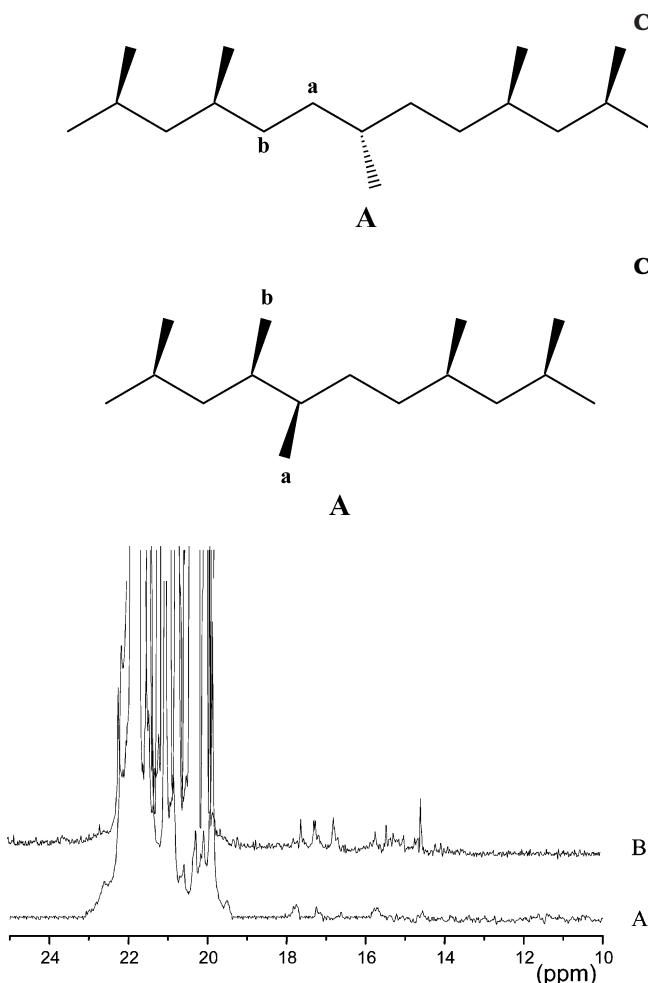


Figure 4. Methyl region of the 50.3 MHz ¹³C NMR spectra of the "isotactic" fraction (A) and of the "less-tactic" fraction (B) of a polypropene-[3-¹³C] sample prepared with catalyst system MgCl₂/TiCl₄-Al(*i*Bu)₃ at 50 °C.

the *m*-S_{αβ} C's), and δ = 35.3–35.8 ppm (including the *r*-S_{αβ} ones).¹⁰

In the spectra of homopolymers, one has to expect that the resonances of the regioirregular sequences are similarly broad and split, with a consequent rise of the threshold for ¹³C NMR detectability. To confirm this guess, we prepared a sample of polypropylene with a 15% enrichment in ¹³C at the methyl C. The methyl region of the ¹³C NMR spectra for the "isotactic" and the "less-tactic" fraction are shown in Figure 4, parts A and B, respectively. In both cases, the resonances of the P_{αβ} and P_{αγ} C's appear as multiplets in the ranges of δ = 14.3–16.0 and 16.5–18.0 ppm. Once again, the pattern is more simple for the "isotactic" fraction, with four main peaks (at δ = 14.6, 15.7, 17.2, and 17.6 ppm) which can be assigned¹¹ to C_a and C_b of Chart 2A, and to C_c and C_d of Chart 2B; this provides further evidence for a substantial lack of stereoselectivity in 2,1-insertion. In the spectrum of the "less-tactic" fraction, additional peaks in the ranges of δ = 15.3–15.8 and 16.3–16.5 ppm can be traced to similar regiodefects embedded in stereoirregular sequences.¹¹

Despite the ¹³C enrichment, the signal-to-noise ratio was too low for a reliable integration of individual peaks. Moreover, one has to keep in mind that resonances of chain ends also fall in the 14–18 ppm region^{12,13} and that in propene homopolymerization (i.e., in the absence of ethene) a significant fraction of 2,1-insertions may

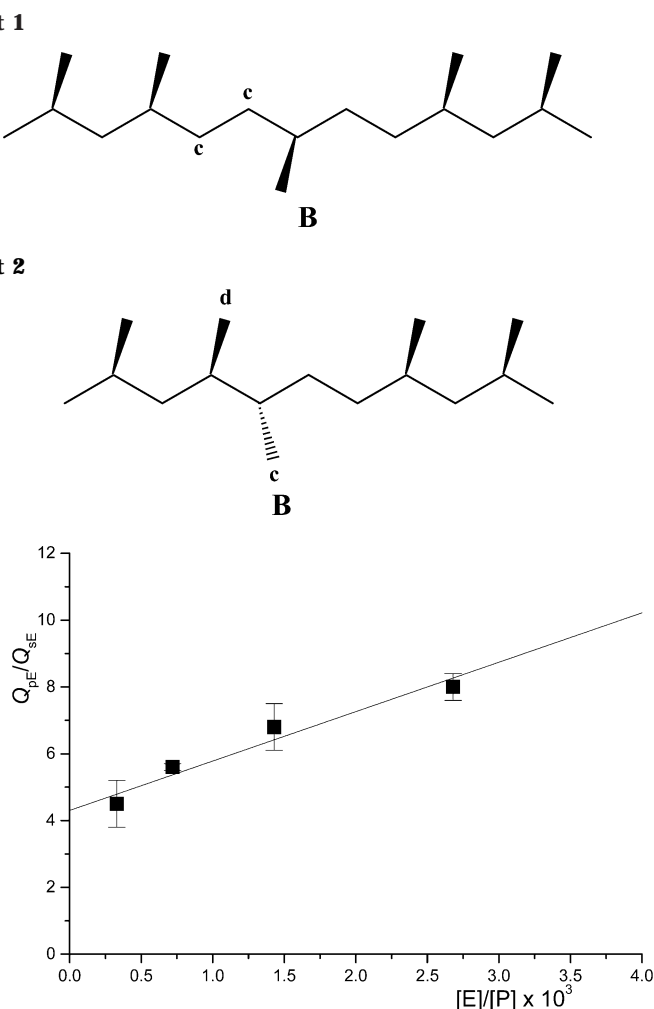


Figure 5. Ratio of ethene-[1-¹³C] units following a 1,2- or a 2,1-propene unit (Q_{pE}/Q_{sE}) vs comonomer feeding ratio in the liquid phase ($[E]/[P]$) for the raw propene/ethene-[1-¹³C] copolymer samples (data from Table 2).

be followed by chain transfer.¹² All this notwithstanding, the cumulative integral of the said region (relative to the total methyl one) was estimated to be 0.4% and 1.4% for the "isotactic" and the "less-tactic" fraction, respectively, which is in reasonable agreement with the much more accurate measurements of regioselectivity based on propene/ethene-[1-¹³C] copolymerization (Table 2).

A fundamental issue to be addressed is the "dormancy" of the growing chains consequent to the regioirregular insertions. In part 1,¹ we demonstrated that—at least for a single-center catalyst—plotting the ratio Q_{pE}/Q_{sE} ($Q_{pE} = Q_E - Q_{sE}$) as a function of Q_E gives a straight line, which intercepts the ordinate axis at $(Q_{pE}/Q_{sE})_0 = (k_{sp}/k_{ps})(k_{pE}/k_{sE})$ (for the definition of all kinetic constants, refer to Scheme 1). The ratio k_{sp}/k_{ps} , in turn, is related to the mole fraction of "dormant" centers (x_d^*) by the following simple equation:^{1,2}

$$x_d^* = (1 + k_{sp}/k_{ps})^{-1}$$

In Figure 5, Q_{pE}/Q_{sE} is plotted vs Q_E for the MgCl₂/TiCl₄-Al(*i*Bu)₃ system. Despite the multisite nature of the catalyst, the plot is linear, and we can assume that the value of $(Q_{pE}/Q_{sE})_0 = 4$ is an average of $(k_{sp}/k_{ps})(k_{pE}/k_{sE})$ over the whole population of catalytic species. For the closely related system MgCl₂/TiCl₄-AlEt₃, by propene hydro-oligomerization² we measured¹⁴ an average

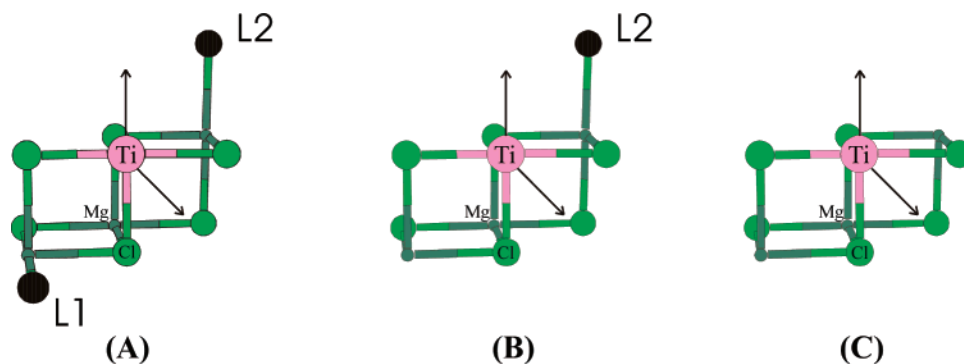


Figure 6. Possible models of active Ti species on the surface of MgCl_2 (see text).

value of $(k_{\text{sp}}/k_{\text{ps}})(k_{\text{pH}}/k_{\text{sH}}) = 1.0$ (once again, for the definitions see Scheme 1).

Unfortunately, there is no way to measure independently the two factors of the products $(k_{\text{sp}}/k_{\text{ps}})(k_{\text{pE}}/k_{\text{sE}})$ and $(k_{\text{sp}}/k_{\text{ps}})(k_{\text{pH}}/k_{\text{sH}})$.¹ Due to the small size of the C_2H_4 and H_2 molecules, one may assume that they do not “feel” the different steric hindrance with growing chains with a last-inserted 1,2- or 2,1-propene unit and that, therefore, the two ratios $(k_{\text{pE}}/k_{\text{sE}})$ and $(k_{\text{pH}}/k_{\text{sH}})$ are not far from unity; the fact that for the investigated system it is $k_{\text{pE}}/k_{\text{sE}} \approx 4(k_{\text{pH}}/k_{\text{sH}})$ (similarly to what found for metallocenes¹) is in qualitative agreement with the said guess, but proves at the same time that at least one of the two ratios is not exactly 1. In the absence of additional information, we can only assume that, for the system under investigation, on average it is

$$1.0 \leq k_{\text{sp}}/k_{\text{ps}} \leq 4$$

and that therefore:

$$0.2 \leq x_{\text{d}}^* \leq 0.5$$

A value of $x_{\text{d}}^* = 0.5$ can give reason for an H_2 -induced activation effect of the order of 100%, which is not far from what observed experimentally.¹⁵

(ii) Computer Modeling of Catalytic Species. For over 3 decades, modeling the active species in heterogeneous Ziegler–Natta catalysts for polypropylene has been inspired by a crystallochemical vision, dating back to Cossee¹⁶ and elaborated on by Allegra¹⁷ and by Corradini and co-workers.^{7,18} This approach had the formidable merit to introduce a rationale into a field dominated by empiricism, and elegant crucial experiments by Zambelli¹⁹ confirmed its soundness. The basic assumption is that the structure of the active surfaces can be derived from that of the bulk. In particular, Corradini and co-workers¹⁸ were the first to apply molecular mechanics (MM) to models of epitactic catalytic species on plausible side edges of “violet” TiCl_3 and MgCl_2 crystals (**A** and **B** in Figure 6; **L1** and **L2** = Cl), and to explain their possible stereoselectivity in terms of what is now known as “growing chain orientation mechanism”: the polymer chain, in at least one of the two available coordination sites, would be bound to assume a chiral orientation by steric interactions with the nearest of the two Cl atoms **L1** and **L2** in Figure 6, and this would favor in turn 1,2-propene insertion with the enantioface pointing the methyl group anti to the first chain C–C bond.

In recent years, a modified and extended version of Corradini’s model was elaborated in our group,²⁰ moving from results of high-field ^{13}C NMR microstructural

polymer analysis. According to this version, ligands **L1** and **L2** can also be Lewis base or Al–alkyl molecules, and their coordination can be labile, possibly resulting in a reversible interconversion of species **A**, **B**, and **C** of Figure 6. This can explain the observed formation of highly isotactic, “isotactoid” and syndiotactic sequences/blocks (ascribed to species **A**, **B**, and **C**, respectively).

Clear steric factors favoring 1,2- over 2,1-insertion never did emerge at the MM level on “preinsertion intermediates” for any such model,¹⁸ and it was speculated that the regioselectivity is to be traced to electronic effects and/or to steric interference of the methyl group of propene with the two equatorial collinear Cl–Ti–Cl bonds at some later stage along the 2,1-insertion path; the latter argument has recently received some support from calculations using paired interacting orbital (PIO) analysis.²¹

We decided it timely to examine the model species **A** of Figure 6 with a fully quantum mechanics (QM) approach (see Experimental Section). Optimized geometries for the transition structures corresponding to the favored 1,2- and 2,1-insertions into a primary growing chain (simulated with an ^tBu group) at a catalytic center of Δ configuration are shown in Figure 7.

In accordance with Corradini’s mechanism, the lowest energy insertion path is that of Figure 7A, with the first chain C–C bond pointing away from **L1** (or **L2**), and propene in 1,2-orientation with the methyl substituent anti to the said bond; for a Ti center of the chosen configuration, this corresponds to insertion with the *re* enantioface. Relative to this, the activation energy for 2,1-insertion with the *si* enantioface (Figure 7B) was calculated to be higher by $\Delta E_{\text{regio}}^{\ddagger} \approx 2$ kcal/mol, whereas 2,1-insertion with the *re* enantioface turned out to be not viable due to strong steric repulsion between the methyl group of propene and either **L1** or **L2** (Figure 7C).

This QM value of $\Delta E_{\text{regio}}^{\ddagger}$ agrees within error limits with the *average* experimental one. However, to explain the poor stereoselectivity of 2,1-insertion desumed from the ^{13}C NMR characterizations of homo- and copolymers (see previous section), one needs to conclude that a major contribution to the generation of regiodefects is due to active species in which at least one of the two ligands **L1** and **L2** is missing (i.e., **B** and/or **C** of Figure 6). Such a conclusion seems very reasonable for a donor-free catalyst like the one examined here, known to produce predominantly “isotactoid” and syndiotactic sequences.

Conclusions

The propene/ethene-[1- ^{13}C] copolymerization method¹ has been successfully applied to measure precisely the

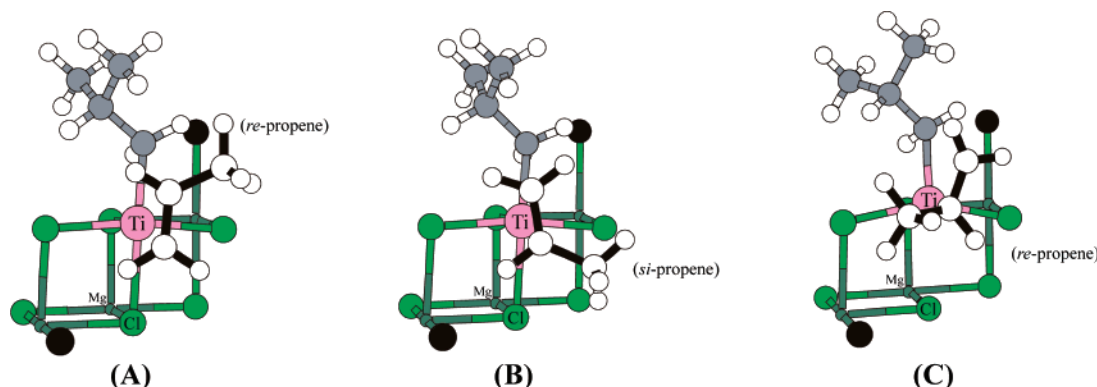


Figure 7. Optimized geometries corresponding to the transition states for the favored (*re* enantioface) 1,2-propene insertion (**A**), and for the two possible 2,1-insertions (*si* enantioface, **B**; *re* enantioface, **C**) at a C_2 -symmetric model site (**A** of Figure 6; **L1** = **L2** = Cl) with Δ configuration. The primary growing chain is simulated with an ⁴Bu group.

regioselectivity in propene polymerization of the “simple” $MgCl_2/TiCl_4$ catalyst (activated with $Al(iBu)_3$), which can be viewed as the ancestor of all present-day $MgCl_2$ -supported industrial catalysts containing Lewis bases as selective modifiers (examined in a forthcoming paper).

It has been found that the average content of 2,1-regiomistakes in the polypropylene produced is fairly high (ca. 0.7 mol %), although—not unexpectedly, due to the multisite catalyst nature—these are distributed rather nonuniformly throughout the polymer. The difficulty in detecting the 2,1-units in the ¹³C NMR spectra of homopolymer samples at natural ¹³C abundance, despite their relatively high concentration, has been traced to their occurrence in a variety of stereochemical environments, which leads to splitting and broadening of the corresponding resonances.

From propene/ethene-[1-¹³C] copolymerization and propene hydro-oligomerization data, the fraction of “dormant” polypropylene chains with a 2,1-last-inserted unit was estimated to be in the 20–50% range.

QM calculations of regioselectivity on classical Corradini-type models of epitactic octahedral catalytic Ti species turned out to be in basic agreement with the experiment.

Experimental Part

Catalyst Preparation and Characterization. A 40 mL sample of a 1.0 M solution of $MgBu_2$ in heptane (Aldrich) was treated in a 250 mL flask with anhydrous $HCl(g)$ for 30 min at room temperature. After purging with flowing argon for 1 h, the suspension was filtered and the pale-yellow finely divided solid washed several times with dry pentane and vacuum-dried; yield, 3.29 g. The solid was then treated twice with excess $TiCl_4$ (80 mL) at 60 °C under vigorous stirring, filtered, washed with three aliquots (50 mL) of dry heptane at 60 °C, and vacuum-dried; yield, 2.93 g. Elemental analysis of the final pale brown solid: Ti, 4.0% (by weight, referred to Ti metal); Cl/Mg mole ratio, 1.7.²² The powder X-ray diffraction profile was collected with a Philips automatic diffractometer with Geiger counter, using Ni-filtered $Cu K\alpha$ radiation, in a custom-made controlled-atmosphere sample cell kept under pure argon.

Propene/Ethene-[1-¹³C] Copolymerization. All propene/ethene-[1-¹³C] copolymerizations were run in a 100 mL jacketed Pyrex reactor, equipped with a magnetic stirrer, a silicone rubber septum, and a gas inlet/outlet, according to the following procedure. The reactor, charged under nitrogen with 50 mL of dry heptane (Aldrich) and 0.2 mL of $Al(iBu)_3$ (Witco GmbH), was thermostated at 50 °C. A gaseous mixture of propene (SON, polymerization grade) and ethene-[1-¹³C] (Isotec

Inc.; 99.9% isotopic purity) at the appropriate composition, prepared with vacuum-line techniques and standardized by gas chromatography, was bubbled through the liquid phase at atmospheric pressure and a flow rate of 0.09 L/min, until gas/liquid equilibrium was attained. The reaction was then started by injecting through the serum cap the catalyst (8.5–8.9 mg), previously suspended in 5.0 mL of dry heptane, and allowed to proceed for 30–45 min, during which the comonomer mixture was kept flowing through the liquid phase at the said rate. Under such conditions, total monomer conversion was lower than 20%, which ensured a nearly constant comonomer feeding ratio. After the reaction was quenched with 5 mL of methanol/HCl (aqueous, concentrated) (95/5 v/v), the copolymer was coagulated with excess methanol/HCl, filtered, washed with more methanol, and vacuum-dried.

Propene-[3-¹³C] Polymerization. Propene-[3-¹³C] (Isotec Inc.; 99.1% isotopic purity), in 15/85 mixture with unlabeled propene, was homopolymerized in a 50 mL jacketed Pyrex reactor, equipped with a magnetic stirrer and a silicone rubber septum, according to the following procedure. First, 25 mL of dry heptane and 0.12 mL $Al(iBu)_3$ were introduced under nitrogen in the reactor, which was thermostated at 50 °C, evacuated with a membrane pump in order to remove nitrogen, and saturated with the monomer mixture at a partial pressure of 1.2 bar. The reaction was started by injecting through the rubber septum the catalyst (12 mg), previously suspended in 5.0 mL of dry heptane, and allowed to proceed at constant monomer pressure for 20 min, after which it was quenched with 5 mL of methanol/HCl (aqueous, concentrated) (95/5 v/v). The polymer (yield, 0.36 g) was then coagulated with excess methanol/HCl, filtered, washed with more methanol, and vacuum-dried.

¹³C NMR Polymer Characterizations. Quantitative ¹³C NMR spectra were recorded with a Varian VXR 200 spectrometer operating at 50.3 MHz, on 100 mg/mL solutions in tetrachloroethane-1,2-*d*₂ at 120 °C. Conditions: 5 mm probe; 76° pulse; acquisition time, 2.0 s; relaxation delay, 1.5 s; 30–60K transients. The spectra were fully simulated with the SHAPE2000 software package.²³

Computational Methods. The calculations of the transition structures shown in Figure 7A–C were performed with the Amsterdam density functional (ADF) program system,²⁴ developed by Baerends et al.²⁵ The electronic configurations of the molecular systems were described by a triple- ζ basis set on titanium for 3s, 3p, 3d, 4s, and 4p. Double- ζ STO basis sets were used for carbon (2s, 2p) and hydrogen (1s), augmented with single 3d and 2p functions, respectively.²⁶ The inner shells on titanium (including 2p) and carbon (1s) were treated within the frozen core approximation. Energetics and geometries were evaluated by using the local exchange-correlation potential by Vosko et al.,²⁷ augmented in a self-consistent manner with Becke's²⁸ exchange gradient correction and Perdew's²⁹ correlation gradient correction (BP86). The geometry of the $MgCl_2$ clusters was kept fixed, with all Mg–Cl distances and all Cl–Mg–Cl angles set equal to 2.50 Å and

90°, respectively. With this computational method, the calculated $\Delta E_{\text{regio}}^{\#}$ value was 1.4 kcal/mol.

To investigate the possible dependence of $\Delta E_{\text{regio}}^{\#}$ on the choice of the functional and on the model size, we carried out the following checks:

(a) On the same model clusters, we repeated the calculations of the transition structures using a hybrid B3LYP^{30,31} functional (in the Gaussian98 program³²). This approach gave $\Delta E_{\text{regio}}^{\#} = 2.0$ kcal/mol.

(b) The ADF calculations were performed for the transition structures of Figure 7A,B on a much larger $\text{Mg}_{13}\text{Cl}_{26}$ cluster, with a TiCl_4 molecule epitactically placed on a 110 cut. The local C_2 -symmetry of the Ti atom was achieved by saturating the two vicinal surface coordination sites with two AlCl_3 units. The calculated $\Delta E_{\text{regio}}^{\#}$ was 1.7 kcal/mol.

Acknowledgment. This work was co-funded by the Italian Ministry for University (PRIN 2002). The ^{13}C NMR polymer characterizations were run at the "Centro di Metodologie Chimico Fisiche" of the University of Naples Federico II, which is also acknowledged for computational time.

References and Notes

- Busico, V.; Cipullo, R.; Ronca, S. *Macromolecules* **2002**, *35*, 1537–1542.
- Busico, V.; Cipullo, R.; Corradini, P. *Makromol. Chem.* **1993**, *194*, 1079–1093.
- Borrelli, M.; Busico, V.; Cipullo, R.; Ronca, S.; Budzelaar, P. H. M. *Macromolecules* **2002**, *35*, 2835–2844.
- Busico, V.; Cipullo, R.; Talarico, G.; Caporaso, L. *Macromolecules* **1998**, *31*, 2387–2390.
- Kissin, Y. V. *Isospecific Polymerization of Olefins*; Springer-Verlag: New York, 1985.
- Moore, E. P. J. *Polypropylene Handbook: Polymerization, Characterization, Properties, Applications*; Hanser Publishers: Munich, Germany, 1996. Chapter 2.
- Corradini, P.; Busico, V.; Guerra, G. *Comprehensive Polymer Science*; Pergamon Press: Oxford, U.K., 1988; Vol. 4, pp 29–50.
- Hayashi, T.; Inoue, Y.; Chujo, R.; Doi, Y. *Polymer* **1989**, *30*, 1714–1722.
- Auriemma, F.; Talarico, G.; Corradini, P. *Progress and Development of Catalytic Olefin Polymerization*; Sano, T., Uozumi, T., Nakatani, H., Terano, M., Eds.; Technology and Education Publishers: Tokyo, 2000, pp 7–15.
- Cheng, H. N.; Smith, D. A. *Macromolecules* **1986**, *19*, 2065–2072.
- Zambelli, A.; Locatelli, P.; Rigamonti, E. *Macromolecules* **1979**, *12*, 156–159.
- Resconi, L.; Cavallo, L.; Fait, A.; Piemontesi, F. *Chem. Rev.* **2000**, *100*, 1253–1346.
- Busico, V.; Cipullo, R. *Prog. Polym. Sci.* **2001**, *26*, 443–533.
- Corradini, P.; Busico, V.; Cipullo, R. *Catalyst Design for Tailor-Made Polyolefins*; Soga, K., Terano, M., Eds.; Kodansha: Tokyo, 1994; pp 21–34.
- Guastalla, G.; Giannini, U. *Makromol. Chem., Rapid Commun.* **1983**, *4*, 519–527.
- (a) Cossee, P. *J. Catal.* **1964**, *3*, 80–88. (b) Arlman, E. J.; Cossee, P. *J. Catal.* **1964**, *3*, 99–104.
- Allegra, G. *Makromol. Chem.* **1971**, *145*, 235–246.
- (a) Corradini, P.; Barone, V.; Fusco, R.; Guerra, G. *J. Catal.* **1982**, *77*, 32–42. (b) Corradini, P.; Barone, V.; Fusco, R.; Guerra, G. *Gazz. Chim. Ital.* **1983**, *113*, 601–607. (c) Corradini, P.; Busico, V.; Cavallo, L.; Guerra, G.; Vacatello, M.; Venditto, V. *J. Mol. Catal.* **1992**, *74*, 433–442. (d) Monaco, G.; Toto, M.; Guerra, G.; Corradini, P.; Cavallo, L. *Macromolecules* **2000**, *33*, 8953–8962.
- (a) Zambelli, A.; Locatelli, P.; Sacchi, M. C.; Rigamonti, E. *Macromolecules* **1980**, *13*, 798–800. (b) Zambelli, A.; Ammendola, P. *Prog. Polym. Sci.* **1991**, *16*, 203–18.
- Busico, V.; Cipullo, R.; Monaco, G.; Talarico, G.; Vacatello, M.; Chadwick, J. C.; Segre, A. L.; Sudmeijer, O. *Macromolecules* **1999**, *32*, 4173–4182.
- Shiga, A. *Micro-Kinetics and Dynamics of Individual Active Sites in Catalytic Reactions*; Terano, M., Otsuka, N., Eds.; Technology and Education Publishers: Tokyo, 2001; pp 119–130.
- See, e.g.: EP 0198151 A2 (priority 22.01.85) to Neste Oy.
- Vacatello, Michele. SHAPE2000 for Windows. University of Naples Federico II (E-mail: vacatello@chemistry.unina.it).
- ADF 2.3.0. Theoretical Chemistry, Vrije Universiteit, Amsterdam, 1996.
- (a) Baerends, E. J.; Ellis, D. E.; Ros, P. *Chem. Phys.* **1973**, *2*, 41. (b) te Velde, B.; Baerends, E. J. *J. Comput. Phys.* **1992**, *99*, 84.
- Snijders, J. G.; Vernooijs, P.; Baerends, E. J. *At. Nucl. Data Tables* **1981**, *26*, 483–509.
- Vosko, S. H.; Wilk, L.; Nusair, M. *Can. J. Phys.* **1980**, *58*, 1200–1211.
- Becke, A. D. *Phys. Rev. A* **1988**, *38*, 3098.
- (a) Perdew, J. P. *Phys. Rev. B* **1986**, *33*, 8822–8824. (b) Perdew, J. P. *Phys. Rev. B* **1986**, *34*, 7406.
- Becke, A. D. *J. Chem. Phys.* **1993**, *98*, 5648.
- Lee, C. Y.; W.; Parr, R. G. *Phys. Rev. B* **1988**, *37*, 785.
- Frisch, M. J.; Trucks, G. W.; Schlegel, H. B.; Scuseria, G. E.; Robb, M. A.; Cheeseman, J. R.; Zakrzewski, V. G.; Montgomery, J. A. J.; Stratmann, R. E.; Burant, J. C.; Dapprich, S.; Millam, J. M.; Daniels, A. D.; Kudin, K. N.; Strain, M. C.; Farkas, O.; Tomasi, J.; Barone, V.; Cossi, M.; Cammi, R.; Mennucci, B.; Pomelli, C.; Adamo, C.; Clifford, S.; Ochterski, J.; Petersson, G. A.; Ayala, P. Y.; Cui, Q.; Morokuma, K.; Malick, D. K.; Rabuck, A. D.; Raghavachari, K.; Foresman, J. B.; Cioslowski, J.; Ortiz, J. V.; Stefanov, B. B.; Liu, G.; Liashenko, A.; Piskorz, P.; Komaromi, I.; Gomperts, R.; Martin, R. L.; Fox, D. J.; Keith, T.; Al-Laham, M. A.; Peng, C. Y.; Nanayakkara, A.; Gonzalez, C.; Challacombe, M.; Gill, P. M. W.; Johnson, B.; Chen, W.; Wong, M. W.; Andres, J. L.; Gonzalez, C.; Head-Gordon, M.; Replogle, E. S.; Pople, J. A. Gaussian, Inc., Pittsburgh, PA, 1998.

MA0341380